EAST EUROPEAN JOURNAL OF PHYSICS. 1. 208-215 (2026)
DOI:10.26565/2312-4334-2026-1-21 ISSN 2312-4334

COMPOSITION AND RADIATION-INDUCED VARIATIONS OF THERMAL CONDUCTIVITY IN $Sn_{1-x}Tb_xSe$ SOLID SOLUTIONS

T.A. Jafarov[1], H.A. Aslanov[1], A.M. Allahverdiyev[1], O.M. Gasanov[1], J.I. Huseynov[1]*, Kh.A. Adgezalova[1], G.A. Garashova[1], I.I. Abbasov[2]

[1]*Azerbaijan State Pedagogical University, Az-1000, Baku, Uz Hajibeyli Str.68, Azerbaijan*
[2]*Azerbaijan State Oil and Industry University,* Az-1010, *Baku, Azadlıq Avenue 20, Azerbaijan*
Corresponding Author email: jahangirhuseynov1958@gmail.com
Received December 4, 2025; revised January 15, 2026; accepted January 25, 2026

In this work, the structural, physicochemical, and thermal transport properties of $Sn_{1-x}Tb_xSe$ ($0 \le x \le 0.05$) alloys were investigated with respect to terbium concentration and γ-irradiation dose. X-ray diffraction and DTA analyses confirmed the formation of orthorhombic substitutional solid solutions following Vegard's law, with a slight increase in lattice parameters and microhardness as Tb content increased. The introduction of Tb atoms into the SnSe matrix enhances phonon–defect scattering due to mass fluctuations and lattice distortions, resulting in a pronounced reduction in thermal conductivity, particularly at low doping levels ($x \le 0.02$). Thermal conductivity measurements performed after γ-irradiation (0–6.5 Mrad, ^{60}Co source) revealed a general decreasing trend for all compositions. In undoped SnSe, the relative decrease reached ~6%, while in Tb-doped samples, the sensitivity to irradiation was significantly reduced. For doses above 5 Mrad, the dependence k(D) is well described by a linear model with high correlation coefficients. These results demonstrate that Tb incorporation not only suppresses phonon transport, enhancing thermoelectric potential, but also increases the radiation resistance of SnSe-based materials.
Keywords: *Thermal conductivity; Phonon scattering; Radiation resistance; γ-irradiation; Solid solutions; Orthorhombic structure; Defect formation; Thermoelectric materials; Lattice distortion; Mass fluctuation scattering*
PACS: 71.20.Nr, 72.20.Pa, 61.72.-y

1. INTRODUCTION

Compounds of the A_4B_6 type ($A = Ge, Sn, Pb$; $B = S, Se, Te$) crystallize in an orthorhombic layered structure (space group *Pnma*), characterized by alternating atomic double layers held together by relatively weak interlayer interactions. This layered configuration gives rise to pronounced anisotropy in their mechanical and electro-optical properties: elastic moduli and dielectric permittivity differ significantly along and across the layers [1]. Electronic structure calculations show that these compounds exhibit narrow or medium band gaps with an indirect transition, making them promising semiconductor materials [2].

A_4B_6 materials exhibit distinct optical responses: calculated functions of dielectric permittivity, energy loss, and the effective number of valence electrons confirm their potential application in optoelectronic devices such as photovoltaic cells, photodetectors, and elements of flexible electronics [3]. Their structural and electronic characteristics also enable control over the anisotropy of charge transport within functional layers.

Tin selenide ($SnSe$) crystals possess a wide range of optical and photoelectric properties determined by their anisotropic layered structure and narrow band gap ($\sim 1.0\ eV$), making them promising materials for infrared optoelectronics [4, 5]. Due to their strong absorption in the visible and near-infrared regions, $SnSe$ can be effectively utilized as a photonic absorber in solar cells and photodetectors [6]. The high carrier mobility and stability of its crystal lattice further enhance its potential for use in photodetectors, solar energy converters, and energy storage devices [7, 8]. Moreover, the combination of high thermoelectric efficiency and sensitivity to light irradiation makes $SnSe$ a versatile material for multifunctional energy-efficient sensors [9].

Enhancement of the thermoelectric parameters of $SnSe$ crystals can be achieved by introducing various dopant impurities, which modify the carrier concentration and phonon-scattering behavior. Doping with rare-earth elements helps optimize the balance between electrical conductivity and thermal conductivity, thereby improving the thermoelectric efficiency of the material [10, 11].

The study of the combined effects of doping and ionizing radiation is a relevant research direction aimed at developing stable and highly efficient thermoelectric materials based on $SnSe$. Alloys of the type $Tb_xSn_{1-x}Se$, derived from $SnSe$, are considered promising thermoelectric materials due to their high Seebeck coefficient and low thermal conductivity. In this work, the dependence of the thermal conductivity of these alloys on the *Tb* content and absorbed dose of gamma irradiation is investigated.

2. EXPERIMENTAL SECTION

For the synthesis of $Sn_{1-x}Tb_xSe$ alloys, high-purity starting materials were used: tin of grade "B4-000", selenium of grade "OC417-4", and chemically pure terbium (99.98%). The synthesis was carried out in evacuated quartz ampoules at a pressure of $0.1333\ Pa$ by a two-stage direct fusion method.

Cite as: T.A. Jafarov, H.A. Aslanov, A.M. Allahverdiyev, O.M. Gasanov, J.I. Huseynov, Kh.A. Adgezalova, G.A. Garashova, I.I. Abbasov, East Eur. J. Phys. 1, 208 (2026), https://doi.org/10.26565/2312-4334-2026-1-21

At the first stage, the ampoule containing the mixture was heated at a rate of $4-5\ ^\circ C$ per minute up to the melting point of selenium and held at this temperature for $3-4\ hours$. Subsequently, the temperature was gradually increased to $950-1000\ ^\circ C$ (depending on the alloy composition) and maintained for $8-9\ hours$ [12].

The interaction in the $SnSe-TbSe$ system was studied using differential thermal analysis (DTA), X-ray phase analysis (XRD), microstructural analysis (MSA), as well as through measurements of microhardness and density [13]. Thermal effects and phase transitions of the obtained samples were investigated by DTA using a *PerkinElmer Simultaneous Thermal Analyzer STA 6000* (USA). Nitrogen was used as the purge gas at a flow rate of 20 mL/s, and the samples were heated up to the melting temperature at a rate of $5\ ^\circ C/min$.

X −ray diffraction (XRD) analysis was performed on a *Rigaku Miniflex* diffractometer operating at 30 kV and 10 mA, using CuKα radiation (λ = 1.5406 Å). The diffraction patterns were recorded within the 2θ range of 0–80° [14]. The morphology and microcomposition of the sample surfaces were examined using a *JEOL JSM-6610LV* scanning electron microscope (Japan).

The thermal conductivity of the investigated samples was measured by an absolutely steady-state method according to the procedure described in [15]. This method provides high accuracy in determining the thermal conductivity coefficient by establishing a stable temperature gradient between the heated and cooled ends of the sample. The measurement error did not exceed 4.2%, confirming the reliability of the obtained experimental data.

For irradiation of samples with different compositions, an ionizing γ-radiation source based on the isotope ^{60}Co was used, with a dose rate of $0.6\ Gy/s$ and photon energy of $1.25\ MeV$. During irradiation, the samples were exposed to radiation at the given dose rate and various absorbed doses for durations of $\boldsymbol{t} = 5, 10, 15, 20, 25$ and $30\ hours$. After irradiation, the thermal conductivity of the samples was measured at a temperature of $\boldsymbol{T} = 300\ K$. A comparative analysis of results obtained before and after irradiation enabled evaluation of the material's radiation resistance.

3. RESULTS AND DISCUSSION

3.1. Physicochemical Analysis

The thermograms of the $Tb_xSn_{1-x}Se$ alloys exhibit distinct peaks upon heating and cooling, corresponding to melting and solidification temperatures, which indicates the formation of congruently melting alloys. Partial substitution of Sn with Tb leads to a decrease in the melting temperature due to lattice deformation and weakening of interatomic bonds. At a $TbSe$ content up to $0.03\ mol.\%$, the microhardness of the samples reaches approximately $500\ MPa$.

Analysis of X −ray diffraction (XRD) patterns shows that the sample is single-phase and exhibits a preferred crystal orientation. Indexing of the diffraction peaks corresponds to an orthorhombic symmetry with space group $D_2h^{16}-Pcmn$ (Fig. 1). Within the composition range $0 \le x \le 0.05$, no noticeable shift of diffraction lines is observed, but their intensity changes, indicating the formation of solid solutions based on $SnSe$. Substitution of Sn atoms with rare-earth elements of larger ionic radii causes a reduction in reflection intensity and a linear increase in lattice parameters, with no deviation from Vegard's law detected.

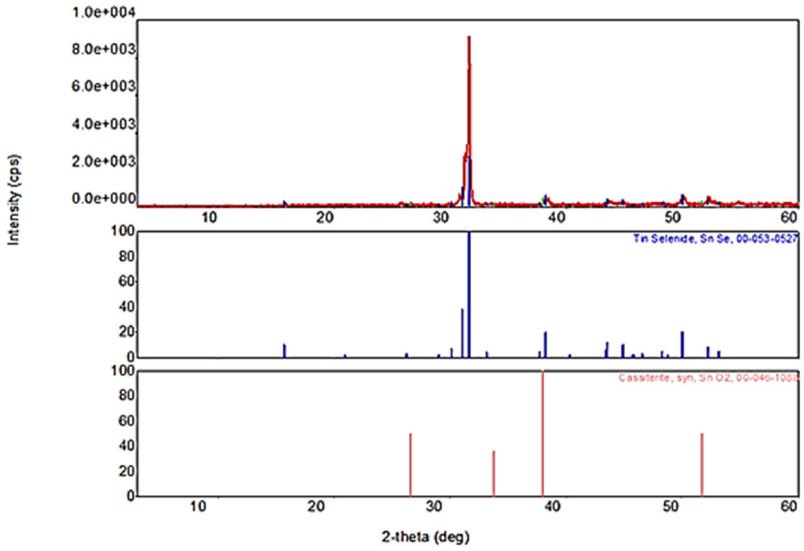

Figure 1. X-ray diffraction spectrum of crystals $Tb_xSn_{1-x}Se$:x = 0.0025. Below are X-ray diffraction patterns of SnSe and SnO for comparison

X −ray structural analysis reveals that the incorporation of terbium selenides leads to an increase in the unit cell parameters of $SnSe$ as the Tb concentration rises. This results in enhanced scattering of charge carriers due to lattice distortions, which correlates with the observed decrease in the thermal conductivity of the alloys [16]. At the same time, the density of $Tb_xSn_{1-x}Se$ compounds remain nearly constant, suggesting that Tb atoms occupy interstitial positions and generate Frenkel-type defects [17].

The increase in lattice parameters and the consistent substitution of *Sn* atoms by *Tb,* along with adherence to Vegard's law, indicate the formation of a substitutional solid solution based on *SnSe*. According to $X-$ray diffraction and pycnometric measurements, the solubility limit of $TbSe$ in $SnSe$ at room temperature is about 5 $mol.\%$.

Comprehensive physicochemical analysis demonstrates that the $Tb_xSn_{1-x}Se$ solid solutions retain an orthorhombic symmetry similar to that of the parent $SnSe$ compound. With increasing $TbSe$ content, a slight increase in lattice parameters, density, and microhardness is observed, along with a shift of thermal effects toward lower temperatures. The difference in electronic configurations between *Sn* and *Tb* atoms leads to distortions in the $SnSe$ crystal lattice upon substitution; however, its fundamental structure remains preserved [18].

Atomic force microscopy (AFM) studies of the surface morphology of $Tb_xSn_{1-x}Se$ crystals reveal a distinctly nonuniform surface with an average roughness of about 25 nm. Such microrelief structures are associated with weak van der Waals interlayer interactions typical of layered compounds. The cleavage of these crystals leads to the formation of separate atomic clusters and microsteps, giving the surface an uneven, wave-like texture. $X-$ray microanalysis (Fig. 2) enabled determination of the phase composition and spatial distribution of the constituent elements. It was found that the surface remains chemically homogeneous overall, although a slight excess of selenium content is observed within the homogeneity region of the $SnSe$ compound.

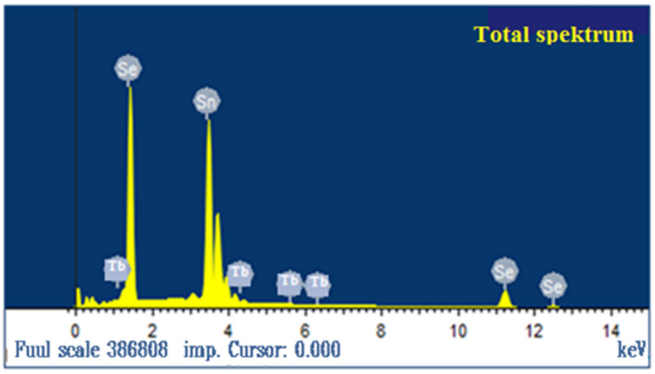

Element	Weight %	Atomic %
Sn L	59.69	49.72
Se L	39.90	50.03
Tb L	0.41	0.25
Total	100	100

Figure 2. X-ray microanalysis of the crystal surface $Tb_xSn_{1-x}Se$:(x=0,005)

3.2. Dependence of Thermal Conductivity on Composition

The thermal conductivity of the system alloys $Sn_{1-x}Tb_xSe$ at room temperature was experimentally determined, and its dependence on the molar fraction of Tb atoms was investigated. According to the experimental results, a clear dependence of the thermal conductivity coefficient (k) on the molar content of Tb was established (Fig. 3).

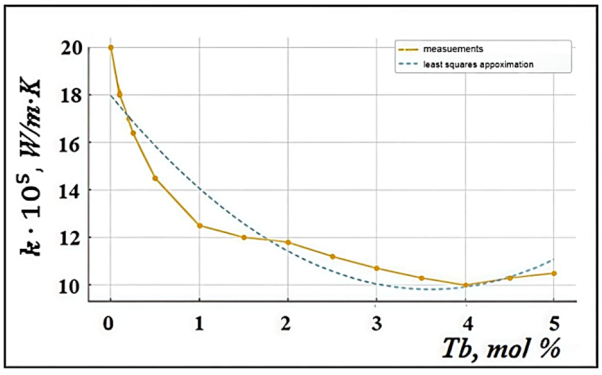

Figure 3. Composition dependence of thermal conductivity in $Sn_{1-x}Tb_xSe$ system alloys

As seen from the graph, the thermal conductivity decreases with increasing Tb concentration, and this reduction is particularly sharp up to approximately 2 $mol\%$. Such behavior is primarily attributed to the increase in defect density and mass fluctuation within the crystal lattice caused by the substitution of Tb atoms into the $SnSe$ matrix. The introduction of Tb enhances phonon scattering [19]. The appearance of Tb nuclei and atoms with different masses reduces the average phonon mean free path, leading to a decrease in thermal conductivity. The rate of reduction is especially high at low Tb concentrations, since the initial doping introduces new scattering centers in the lattice, sharply decreasing the phonon mean free path and consequently the thermal conductivity.

A slight increase in thermal conductivity observed in the range of 4–5 mol%$(10.0 - 10.5) \times 10^{-5} W \cdot m^{-1} \cdot K^{-1}$,is statistically insignificant and most likely results from measurement uncertainties or microstructural variations between samples. The weak increase in this range may also be associated with the formation of a secondary phase or local ordering of the crystal structure at higher Tb contents. Such a dependence can be explained by changes in the material's heat transport mechanisms as the composition changes.

Overall, the conducted studies show that the incorporation of Tb atoms into the $SnSe$ matrix significantly enhances phonon scattering mechanisms, resulting in a pronounced decrease in thermal conductivity. Thus, with increasing Tb concentration in $Sn_{1-x}Tb_xSe$ alloys, heat transfer becomes limited by diffusive phonon scattering, which is of both scientific and practical importance for improving the thermoelectric efficiency of such materials.

In solids, thermal conductivity depends on multiple parameters, and the total thermal conductivity coefficient can be represented as the sum of several major components, which are separated according to the nature of heat carriers in the material [20]:

$$k_{tot} = k_{ph} + k_{el} + k_{ex} + k_{maq} + k_f + k_{bp}$$

For semiconductors, the thermal conductivity is usually expressed as the sum of two main parts [21]:

$$k_{tot} = k_{ph} + k_{el},$$

where k_{ph} −is the phonon (lattice) contribution, i.e., the heat flux carried by atomic vibrations (phonon propagation), and k_{el} − is the electronic contribution, i.e., the heat flux carried by free charge carriers (electrons and holes).

The electronic thermal conductivity can be approximately estimated using the Wiedemann–Franz law [22]:

$$k_{el} = L\sigma T,$$

where L −is the Lorenz constant ($\approx 2.44 \cdot 10^{-8} W\Omega K^{-2}$for ideal metals, but variable for semiconductors depending on band structure), $\sigma$is the electrical conductivity, and T is the absolute temperature.

Calculations show that in $SnSe$ −based semiconductors, heat transport is predominantly phononic, and the low thermal conductivity of such compounds is mainly due to strong phonon scattering [23]. The partial substitution of Sn atoms by Tb atoms break the local symmetry of the crystal lattice and creates point defects. These defects increase the probability of elastic phonon scattering, thereby reducing the thermal conductivity.

The mechanism of phonon–defect scattering can be described by the Clemens model [24]. According to this model, the average phonon lifetime limited by point-defect scattering decreases as follows:

$$\tau_{pd}^{-1} \propto \Gamma\omega^4,$$

where $\Gamma = {}_i f_i(1 - M_i/M_{av})^2$is the mass-fluctuation parameter, $\omega$is the phonon frequency, M_i and M_{av} are the atomic masses of the components and their average atomic mass, respectively.

The substitution of Sn atoms with Tb introduces differences not only in mass but also in elastic modulus, which shortens the phonon mean free path and lowers the thermal conductivity. This model successfully explains the sharp decline in thermal conductivity observed in the range of $0 - 3\ mol\%\ Tb$.To provide a more complete description of heat transport in the alloys, the Callaway model [25] was employed. According to this model, the thermal conductivity is determined by the combined influence of several scattering mechanisms. The total phonon relaxation rate is given by Matthiessen's rule [26]:

$$\tau_C^{-1} = \tau_U^{-1} + \tau_B^{-1} + \tau_{pd}^{-1},$$

where τ_U^{-1} − corresponds to Umklapp scattering processes, τ_U^{-1} −represents boundary scattering, and τ_{pd}^{-1} − accounts for point-defect scattering.

As the Tb concentration increases, the intensity of point-defect scattering rises (i.e., τ_{pd}^{-1}increases), which shortens the total phonon lifetime and leads to a monotonic decrease in the thermal conductivity of the samples.

The observed compositional dependence of thermal conductivity can also be explained by the Clemens–Abeles alloy model, which attributes the enhanced phonon scattering to increasing differences in the masses and radii of the constituent atoms, resulting in reduced thermal conductivity [27].

According to the experimental data, the slight rise in thermal conductivity at $4 - 5\ mol\%$ Tb, although statistically insignificant, may be related to local microstructural modifications or the formation of a secondary phase (e.g., Tb_2Se_3).

In conclusion, the obtained experimental results demonstrate that the thermal conductivity of $Sn_{1-x}Tb_xSe$ alloys is primarily governed by phonon–defect scattering mechanisms. Increasing Tb concentration enhances lattice disorder, decreases the phonon mean free path, and consequently reduces the overall thermal conductivity. This relationship is fully consistent with both the Clemens and Callaway models.

3.3. Dependence of Thermal Conductivity on the Absorbed Radiation Dose

To investigate the effect of ionizing radiation on the thermal conductivity of the $Sn_{1-x}Tb_xSe$ alloy system, samples with compositions $x = 0;\ 0.001;\ 0.01;\ 0.025;$ and 0.05 were synthesized and subjected to γ −irradiation in the dose

range of $0 - 6.5\ Mrad$. For each dose, the thermal conductivity (k) was measured, and the obtained results are summarized in Table 1.

It follows from Table 1 that within the investigated dose interval ($0 - 6.5\ Mrad$), the thermal conductivity of $Sn_{1-x}Tb_xSe$ alloys under γ-irradiation exhibits a general decreasing trend for all compositions. The largest relative change is observed in the undoped sample ($x = 0$), where$\Delta k/k_0 \approx -6\%$. This indicates that in pure $SnSe, \gamma$ −irradiation enhances phonon scattering more strongly than in doped alloys. With increasing Tb concentration, the decrease in k becomes progressively weaker, reaching only -1.38% at $x = 0.05$. This effect can be attributed to the fact that Tb incorporation initially suppresses phonon scattering in the crystal lattice, partially compensating for the influence of additional radiation-induced defects.

Table 1. Thermal conductivity of $Sn_{1-x}Tb_xSe$ system alloys at different absorption doses

Absorbed dose D, Mrad	COMPOSITIONS				
	x=0	*x=0.001*	*x=0.01*	*x=0.025*	*x=0.05*
	k·10^{-5}, W/(m^{-1}K^{-1})	**k·10^{-5}, W/(m^{-1}K^{-1})**	**k·10^{-5}, W/(m^{-1}K^{-1})**	**k·10^{-5}, W/(m^{-1}K^{-1})**	**k·10^{-5}, W/(m^{-1}K^{-1})**
0	20	18	12.5	11.2	14.5
1	20	18	12.5	11.2	14.5
2	20	18	12.5	11.2	14.5
3	20	18	12.5	11.2	14.5
4	20	18	12.5	11.2	14.5
5	19.8	17.9	12.5	11.2	14.5
5,5	19.5	17.7	12.4	11.2	14.5
6	19.2	17.4	12.3	11.1	14.4
6.5	18.8	17.1	12.2	11.0	14.3

The dependences of thermal conductivity on the γ-irradiation dose for different compositions are shown in Figure 4. These plots demonstrate that the $k(D)$ behavior is consistent with a radiation defect accumulation model, in which increasing defect concentration enhances phonon scattering. At low doses, k remains nearly constant; however, once a threshold dose is reached, thermal conductivity begins to decrease monotonically.

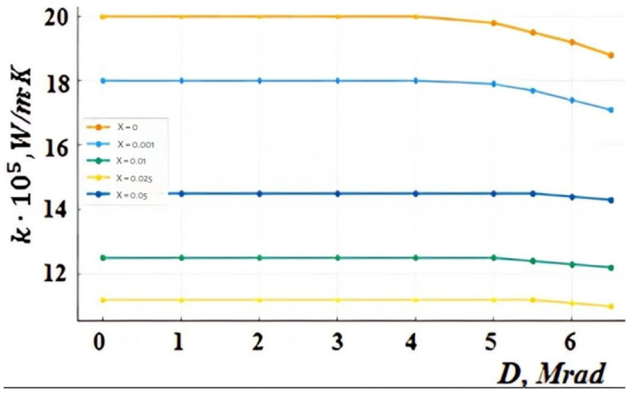

Figure 4. Dependence of thermal conductivity in $Sn_{1-x}Tb_xSe$ system alloys on absorption dose

Mathematically, this behavior can be described using two main approaches:

1. Exponential saturation model:$N(D) = N_\infty(1 - e^{-\sigma D})$ −where *N(D)* is the defect concentration increasing with dose *D* and approaching saturation. The corresponding expression for thermal conductivity is [28]:

$$k(D) = k_\infty + (k_0 - k_\infty)e^{-\alpha D}$$

where $k_0 = k(0), k_\infty -$ is the asymptotic value at large doses, and α is the accumulation-rate parameter. This model is often applied to describe the influence of vacancy (or cluster) buildup on phonon scattering.

2. Threshold-linear (empirical) model: For cases where the material remains nearly unchanged at low doses and shows an approximately linear decrease beyond a threshold [29]:

$$k(D) = \begin{cases} k_0 \ D \le D_{th} \\ a + bD \ D > D_{th} \end{cases}$$

where D_{th} is the threshold dose ($\approx 5\ Mrad$), a is the extrapolated initial value, and $b < 0$ is the slope characterizing the sensitivity of thermal conductivity to radiation dose.

This model is convenient for limited dose ranges exhibiting a clear defect activation threshold (e.g., defect clustering or local structural transitions). In studies of ionizing radiation effects, this empirical approach is frequently employed for analyzing low- and medium-dose regimes.

Experimental data for $Sn_{1-x}Tb_xSe$ alloys show that within $D = 0-5\ Mrad$, no significant change in k occurs. However, at $D = 5-6.5\ Mrad$, the decrease becomes pronounced. The analysis indicates that in this active region, $k(D)$ is well described by a linear dependence,$(k(D) = a + bD)$ (Figure 5). The obtained parameters and statistical measures are given in Table 2.

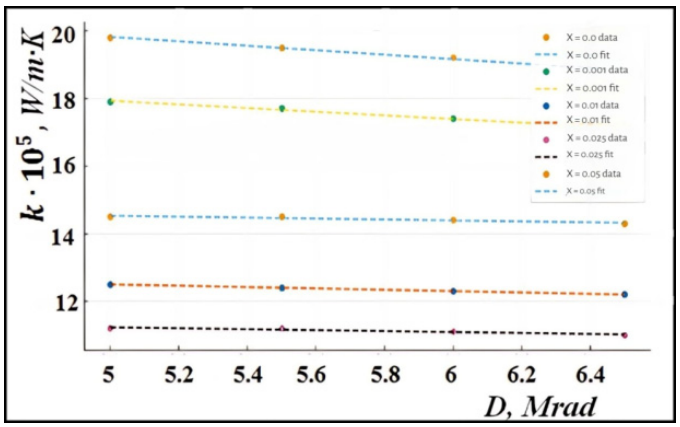

Figure 5. Active-range (5.0-6.5 Mrad) with linear fits

Table 2. Linear approximation parameters and statistical indicators

Composition	Slope b (k per Mrad)	Slope standard error	Intercept A (k units)	Intercepts	R^2	RMSE
x=0	−0.6600	0.0346	23.1200	0.2001	0.9945	0.0274
x=0.001	−0.5400	0.0346	20.6300	0.2001	0.9918	0.0274
x=0.01	−0.2000	0.0000	13.5000	0.0000	1.0000	0.0000
x=0.025	−0.1400	0.0346	11.9300	0.2001	0.8909	0.0274
x=0.05	−0.1400	0.0346	15.2300	0.2001	0.8909	0.0274

As seen from Table 2, the correlation coefficient $R^2 \approx 0.99$ for most compositions, indicating excellent agreement between the experimental data and the linear model. This confirms that the decrease in thermal conductivity follows an almost perfectly linear law. In particular, for $x = 0.01$, the coefficient $R^2 = 1.0000$, showing an ideal fit.

For all compositions, the slope b is negative $(b < 0)$, meaning that thermal conductivity decreases with increasing γ-irradiation dose. Moreover, as the Tb content increases, the absolute value of b decreases, indicating a reduction in the sensitivity of thermal conductivity to radiation. The low standard errors of the slopes $(\sim 0.03-0.04)$ and small RMSE values $(0.027-0.03)$ confirm the statistical reliability and accuracy of the linear fit.

Thus, for all $Sn_{1-x}Tb_xSe$ alloys, the thermal conductivity decreases with increasing γ −irradiation dose, with the strongest effect observed in pure $SnSe$. As Tb concentration increases, the alloys' radiation resistance increases, and the rate of decrease in k weakens. Experimental results indicate that within $D = 0-5\ Mrad$, $k$remains nearly constant, whereas for $D > 5\ Mrad$, it follows a clear linear dependence described by $k(D) = a + bD$. The reduction in the absolute value of negative slopes with higher Tb content reflects the suppression of phonon scattering by Tb ions and partial compensation for radiation-induced defects [30].

CONCLUSIONS

The structural and thermal analyses performed on $Sn_{1-x}Tb_xSe$ alloys demonstrate that terbium incorporation leads to the formation of stable substitutional solid solutions with orthorhombic symmetry preserved across the studied composition range. Increasing Tb content results in moderate lattice expansion, microhardness growth, and enhanced defect-induced phonon scattering, which collectively cause a significant reduction in thermal conductivity, especially at low dopant concentrations.

The study of γ-irradiation effects in the dose range $0-6.5\ Mrad$ revealed that thermal conductivity decreases for all compositions, with the strongest degradation ($\approx 6\%$) observed in undoped $SnSe$. For alloys with higher Tb content, the reduction becomes progressively weaker, indicating improved radiation resistance. For irradiation doses above $5\ Mrad$, thermal conductivity follows a nearly perfect linear decay, accurately described by empirical $k(D) = a + bD$ relations with high correlation coefficients.

Overall, the obtained results confirm that Tb doping effectively suppresses phonon transport while simultaneously enhancing the radiation stability of $SnSe$ −based materials, making $Sn_{1-x}Tb_xSe$ alloys promising candidates for thermoelectric and radiation-resistant semiconductor applications.

ORCID

O.M. Gasanov, https://orcid.org/0000-0003-4888-7686; **J.I. Huseynov,** https://orcid.org/0000-0002-4498-2400;
I.I. Abbasov, https://orcid.org/0000-0001-8111-2642

REFERENCES

[1] H. Koc, S. Simsek, S. Palaz, O. Oltulu, A.M. Mamedov, and E. Ozbay, "Mechanical, electronic, and optical properties of the A4B6 layered ferroelectrics: ab initio calculation," Phys. Status Solidi C, **12**(6), 651–658 (2015). https://doi.org/10.1002/pssc.201400245

[2] L.T. Nguyen, and G. Makov, "Lone-Pair Origins of Polymorphism: Sn Monochalcogenides as a Case Study," Chemistry of Materials, **36**(11), 5487–5499 (2024).https://doi.org/10.1021/acs.chemmater.4c00409

[3] Y. Xu, H. Zhang, H. Shao, *et al*., "Electronic, transport and optical properties of monolayer α and βGeSe: A first-principles study," Phys. Rev. B, **96**, 245421 (2017). https://doi.org/10.1103/PhysRevB.96.24542

[4] L.D. Zhao, S.H. Lo, Y. Zhang, *et al.* "Ultralow thermal conductivity and high thermoelectric figure of merit in SnSe crystals," Nature, **508**, 373–377 (2014). https://doi.org/10.1038/nature13184

[5] Y. Yu, T. Xiong, Z. Guo, *et al*. "Wide-spectrumpolarization-sensitiveandfast-responsephotodetectorbasedon 2D group IV-VI semiconductor tin selenide," Fundamental Research, **2**(6), 985-992, (2022). https://doi.org/10.1016/j.fmre.2022.02.008

[6] Z. Liang, R. Hao, H. Luo, Z. He, L. Su, and X. Fan, "Enhancing the photo-response performance of SnSe-based photoelectrochemical photodetector via Ga doping," Journal of Materials Chemistry C, **12**(8), (2024). https://doi.org/10.1039/D3TC03937D

[7] K. Mukai, R. Wanibuchi, and Y. Nunomura, "Improved performance of solar cells using chemically synthesized SnSe nanosheets as light absorption layers," J. Mater. Sci: Mater. Electron. **35**, 680 (2024).https://doi.org/10.1007/s10854-024-12366-1

[8] B. Qin, D. Wang, T. Hong, *et al*. "High thermoelectric efficiency realized in SnSe crystals via structural modulation," Nat. Commun. **13**(14), 1366 (2023). https://doi.org/10.1038/s41467-023-37114-7

[9] G. Shi, and E. Kioupakis, "Quasiparticle band structures and thermoelectric transport properties of p-type SnSe," J. Appl. Phys. **117**, 065103 (2015). https://doi.org/10.1063/1.4907805

[10] Sh.S. Ismailov, M.A. Musaev, I.I. Abbasov, *et al*. "Effect of doping level and compensation on thermal conductivity in $Ce_xSn_{1-x}Se$ solid solutions," Low Temp. Phys. **46**, 1114–1120 (2020). https://doi.org/10.1063/10.0002155

[11] J.I. Huseynov, and T.A. Jafarov, "The Influence of γ-Irradiation on Thermo emf and Heat Conduction of $Ln_{0.01}Sn_{0.99}Se$ (LnPr, Tb, Er) Monocrystals, World Journal of Condensed Matter Physics, **4**(1) 5 (2014). https://doi.org/10.4236/wjcmp.2014.41001

[12] J.I. Huseynov, M.I. Murguzov, and S.S. Ismayilov, "Specific features of self-compensation in $Er_xSn_{1-x}Se$ solid solutions," Semiconductors, **47**, 323–326 (2013). https://doi.org/10.1134/S106378261303010X

[13] I.I. Aliev, J.I. Huseynov, M.I. Murguzov, *et al*. "Phase relations and properties of alloys in the SnSe-DySe system," Inorg. Mater. **50**, 237–240 (2014).https://doi.org/10.1134/S0020168514030029

[14] I.I. Abbasov, Sh.S. Ismailov, and V.A. Abdurahmanova, "Concentration dependences of electrical conductivity and the Hall effect of the $Ce_xSn_{1-x}Se$ single crystals," Low Temperature Physics, **45**, 1277–1280 (2019). https://doi.org/10.1063/10.0000209

[15] I. Huseynov, M.I. Murquzov, R.F. Mamedova, and Sh.S. Ismailov, "Thermal Conductivity and Thermal EMF of Materials for Thermal Energy Converters," in: *TPE-06 3rd Intern. Conf. on Technical and Physical Problems in Power Engineering*, (Ankara, 2008).

[16] J.I. Huseynov, M.I. Murguzov, Sh.S. Ismailov, R.F. Mamedova, and E.M. Gojayev, "On the thermopower and thermomagnetic properties of $Er_xSn_{1-x}Se$ solid solutions," Semiconductors, **51**(2), 153-157 (2017). https://doi.org/10.1134/S1063782617020075

[17] J.I. Huseynov, M.I. Murguzov, and S.S. Ismayilov, "Specific features of self-compensation in $Er_xSn_{1-x}Se$ solid solutions," Semiconductors,**47**, 323–326 (2013). https://doi.org/10.1134/S106378261303010X

[18] O.M. Hasanov, C.I. Huseynov, H.A. Aslanov, *et al*. "Galvanomagnetic Properties of $Gd_xSn_{1-x}Se$ Solid Solutions," Journal of Baku Engineering University – Physics, **8**(2), 81-90 (2024).https://doi.org/10.30546/09081.2024.102.7068

[19] W.-Y. Lyu, W.D. Liu, M. Li, *et al*. "The effect of rare earth element doping on thermoelectric properties of GeTe," Chemical Engineering Journal, **446(**Part 1), 137278, (2022). https://doi.org/10.1016/j.cej.2022.137278

[20] *Thermal Conductivity: Theory, Properties, and Applications*, edited by Terry M. Tritt, (Springer US, New York, 2004). https://doi.org/10.1007/b136496

[21] Q. Zheng, A.B. Mei, M. Tuteja, *et al*. "Phonon and electron contributions to the thermal conductivity of VN_x epitaxial layers Phys. Rev. Materials,**1**, 065002 (2017). https://doi.org/10.1103/PhysRevMaterials.1.065002

[22] V.N. Glazkov, L. Ginzburg, and A. Orlov, "Wiedemann-Franz law demonstration in a student practicum," Am. J. Phys. **85**, 473-477 (2017).https://doi.org/10.1119/1.4982787

[23] D.I. Huseynov, M.I. Murguzov, and S.S. Ismailov, "Thermal conductivity of $Er_xSn_{1-x}Se$ ($x \leq 0.025$) solid solutions," Inorg. Mater. **44**, 467–469 (2008).https://doi.org/10.1134/S0020168508050063

[24] R. Gurunathan, R. Hanus, M. Dylla, *et al*. "Analytical Models of Phonon–Point-Defect Scattering," Phys. Rev. Applied, **13**, 034011 (2020). https://doi.org/10.1103/PhysRevAppleid.13.034011

[25] J. Callaway, "Model for Lattice Thermal Conductivity at Low Temperatures," Phys. Rev. **113**, 1046, (1959). https://doi.org/10.1103/PhysRev.113.1046

[26] T. Feng, B. Qiu, X. Ruan, "Coupling between phonon-phonon and phonon-impurity scattering: A critical revisit of the spectral Matthiessen's rule," Phys. Rev. B, **92**, 235206 (2015). https://doi.org/10.1103/PhysRevB.92.235206

[27] B. Abeles, "Lattice Thermal Conductivity of Disordered Semiconductor Alloys at High Temperatures," Phys. Rev. **131**, 1906 (1963). https://doi.org/10.1103/PhysRev.131.1906

[28] Y. Zhao, D. Liu, J. Chen, *et al*. "Engineering the thermal conductivity along an individual silicon nanowire by selective helium ion irradiation," Nat. Commun.**8**, 15919 (2017). https://doi.org/10.1038/ncomms15919

[29] W. Zhao, Y-H. Li, H-Z. Ma, *et al*. "Dependence of irradiation defects evolution on dose rate and PKA energy spectrum in tungsten," Nuclear Materials and Energy, **43**, 101956 (2025). https://doi.org/10.1016/j.nme.2025.101956

[30] J.I. Huseynov, and T.A. Jafarov, "Effect of γ-ray radiation on electrical properties of heat-treated $Er_xSn_{1-x}Se$ single crystals," Semiconductors, **46**, 430–432 (2012). https://doi.org/10.1134/S1063782612040082

СКЛАД ТА РАДІАЦІЙНО-ІНДУКОВАНІ ЗМІНИ ТЕПЛОПРОВІДНОСТІ У ТВЕРДИХ РОЗЧИНАХ $Sn_{1-x}Tb_xSe$

Т.А. Джафаров[1], Г.А. Асланов[1], А.М. Аллахвердієв[1], О.М. Гасанов[1], Дж.І. Гусейнов[1], Х.А. Адгезалова[1], Г.А. Гарашова[1], І.І. Аббасов[2]

[1]Азербайджанський державний педагогічний університет, Az-1000, Баку, вул. Уз Гаджибейлі, 68, Азербайджан

[2]Азербайджанський державний університет нафти та промисловості, Az-1010, Баку, проспект Азадлик, 20, Азербайджан

У цій роботі досліджували структурні, фізико-хімічні та термотранспортні властивості сплавів $Sn_{1-x}Tb_xSe$ ($0 \le x \le 0,05$) залежно від концентрації тербію та дози γ-опромінення. Рентгенівська дифракція та ДТА-аналіз підтвердили утворення орторомбічних твердих розчинів заміщення згідно із законом Вегарда, з незначним збільшенням параметрів кристалічної решітки та мікротвердості зі збільшенням вмісту Tb. Введення атомів Tb у матрицю SnSe посилює розсіювання фононів-дефектів через флуктуації маси та спотворення кристалічної решітки, що призводить до помітного зниження теплопровідності, особливо при низьких рівнях легування ($x \le 0,02$). Вимірювання теплопровідності, проведені після γ-опромінення (0–6,5 Мрад, джерело ^{60}Co), виявили загальну тенденцію до зниження для всіх складів. У нелегованому SnSe відносне зниження досягло ~6%, тоді як у зразках, легованих Tb, чутливість до опромінення значно знизилася. Для доз вище 5 Мрад залежність k(D) добре описується лінійною моделлю з високими коефіцієнтами кореляції. Ці результати демонструють, що включення Tb не тільки пригнічує транспорт фононів, посилюючи термоелектричний потенціал, але й підвищує радіаційну стійкість матеріалів на основі SnSe.

Ключові слова: *теплопровідність; розсіювання фононів; радіаційна стійкість; γ-опромінення; тверді розчини; орторомбічна структура; утворення дефектів; термоелектричні матеріали; спотворення кристалічної решітки; розсіювання флуктуацій маси*